IJCRT.ORG ISSN : 2320-2882

INTERNATIONAL JOURNAL OF CREATIVE RESEARCH THOUGHTS (IJCRT)

An International Open Access, Peer-reviewed, Refereed Journal

Design and Implementation of Wind Solar Hybrid Power Plant With EV Charging and Energy Storage

Miss.Bhavana Doifode[1], Dr.Amit Mohod[2], Dr.Krunal Panpaliya[3]

[1]Student, Electrical Engineering Department,id - 0009-0009-8434-2246

Prof. Ram Meghe College of Engineering & Management, Badnera,Amravati,Maharashtra-444701

[2]Professor, Electrical Engineering Department

Prof. Ram Meghe College of Engineering & Management, Badnera, Amravati,Maharashtra-444701

[3]Assistant Professor, Electrical Engineering Department,id - 0009-0001-4702-5374

Prof. Ram Meghe College of Engineering & Management, Badnera, Amravati,Maharashtra-444701

***Abstract*—*This work presents an IoT-enabled hybrid renewable energy charging station designed for electric vehicle applications. The system integrates a 12V/10W polycrystalline solar photovoltaic panel and a 3V DC generator motor functioning as a small-scale Wind Energy Conversion System to address the intermittency challenges inherent in single-source renewable installations. The station employs an ESP32 DevKit V1 microcontroller with dual-core Xtensa 32-bit LX6 processor, integrated 12-bit analog-to-digital conversion capability, and built-in Wi-Fi connectivity. Voltage sensing is accomplished through a precision resistive divider network with R_1 = 30kΩ and R_2 = 7.5kΩ, providing a scaling factor of 5.0 to accommodate input voltages up to 16.5V. Current measurement utilizes an ACS712 Hall Effect sensor offering 2.1 kV RMS galvanic isolation. Power delivery to the electric vehicle is achieved through wireless inductive coupling, eliminating physical connector wear and enhancing safety in adverse weather conditions. The Blynk IoT Cloud platform provides remote monitoring via Virtual Pins V0, V1, and V2 for voltage, current, and power respectively. Experimental results demonstrate stable voltage regulation between 1.87V and 2.03V with consistent current delivery of 0.151A, yielding 0.28W power output. The wireless power transfer mechanism achieves approximately 75% efficiency at an optimal air gap of 5mm. The system represents a unified approach to decentralized electric vehicle charging infrastructure, combining hybrid energy harvesting, contactless power delivery, and IoT telemetry in a single low-cost prototype.*

***Keywords*—*Hybrid renewable energy systems, wireless power transfer, Internet of Things, electric vehicle charging, ESP32 microcontroller, Blynk cloud platform.*

I. INTRODUCTION

Recent advances in automotive technology have enabled a fundamental transformation from internal combustion engine vehicles to battery-electric vehicles, significantly reducing urban air pollution and greenhouse gas emissions. However, the environmental benefits of EV adoption are substantially diminished when charging infrastructure relies predominantly on fossil-fuel-based electrical grids. This contradiction has motivated research into decentralized renewable energy charging stations that can operate independently of conventional grid infrastructure.

Solar photovoltaic systems provide excellent power density during peak daylight hours but become completely ineffective during nighttime operation. Wind energy conversion systems offer complementary generation patterns, often producing maximum output during evening hours or weather conditions that reduce solar irradiance. Thus, the challenge lies in designing circuits that combine these intermittent sources into a reliable hybrid power system.

Current electric vehicle charging infrastructure faces three fundamental limitations: (1) Grid dependency creates substantial load on national electrical distribution networks during peak charging hours; (2) Intermittency, as solar power generation ceases entirely during nighttime while wind patterns exhibit high variability; (3) Physical constraints of conventional wired charging involve mechanical wear of connectors and present electrical safety hazards in wet conditions.

This work describes a hybrid wind-solar charging station utilizing a 12V/10W polycrystalline solar panel and a 3V DC generator motor acting as a small-scale wind turbine, with real-time power monitoring through an ESP32 DevKit V1 microcontroller and wireless power delivery via inductive coupling. The primary goals are: (i) continuous power availability despite individual source intermittency; (ii) high-precision monitoring using the ACS712 current sensor and optimized voltage divider; (iii) IoT telemetry via Blynk platform with latency below 200 ms; (iv) wireless power transmission efficiency above 70% at practical air gap distances.

II. LITERATURE REVIEW

A. Solar Photovoltaic Systems

Solar photovoltaic technology has transitioned from expensive monocrystalline installations to affordable polycrystalline and thin-film applications. Research by Chopra et al. indicates that small-scale photovoltaic panel efficiency ranges between 15% and 20% under standard test conditions. The power output of a photovoltaic panel depends on solar irradiance and temperature according to the single-diode equivalent circuit model:

$$I = I_p^h - I_o [exp(qV/nkT) - 1]$$

where I_p^h is the photo-generated current proportional to irradiance, I_o is the dark saturation current, q is elementary charge, V is the junction voltage, n is the diode ideality factor, k is Boltzmann's constant, and T is absolute temperature.

B. Small-Scale Wind Energy Conversion Systems

Small-scale wind energy conversion systems differ significantly from industrial wind farms. Using a 3V DC generator motor mimics the behavior of a permanent magnet DC generator. The back-electromotive force generated is proportional to the angular velocity:

$$E^g = K^a \cdot \varphi \cdot \omega$$

Schottky diodes with forward voltage drops of 0.2V–0.3V are preferred for low-voltage renewable energy applications to ensure unidirectional power flow with minimal losses.

C. Hybrid Power Systems

A study in the Journal of Renewable Energy concludes that hybrid systems provide a 30% higher reliability index than standalone solar systems when evaluated over annual operational cycles. Solar generation peaks during midday while wind generation often peaks during evening hours, providing temporal complementarity that improves overall system availability. The primary technical challenge in hybrid system design is impedance matching and backflow prevention between sources.

D. Wireless Power Transfer Technologies

Inductive coupling operates at short range (millimeters to centimeters) and achieves efficiency between 80% and 90%, used in consumer electronics and the SAE J2954 standard for EV wireless charging. The mutual inductance between transmitter and receiver coils is:

$$M = k\sqrt{(L_1 L_2)}$$

where k is the coupling coefficient (0 to 1), L_1 and L_2 are coil inductances. The resonant frequency is: $f_r = 1/(2\pi\sqrt{(LC)})$, which maximizes power transfer efficiency by minimizing reactive power circulation.

E. IoT in Power Monitoring

The ESP32 microcontroller is preferred for IoT projects due to its 12-bit ADC offering 4096 discrete levels compared to Arduino's 10-bit (1024 levels). Literature indicates that Blynk's WebSocket protocol provides latency as low as 100ms, vital for detecting voltage surges that could damage connected EVs. While many researchers studied high-power hybrid grids, there is a lack of integrated low-cost prototypes combining hybrid generation, wireless delivery, and IoT telemetry in a unified system. This research fills that gap.

III. SYSTEM DESIGN AND METHODOLOGY

A. Proposed System Architecture

The system is designed as a micro-grid charging station integrating two renewable energy harvesters, a central processing unit, and a contactless power delivery mechanism. The generation stage consists of a solar PV panel and a 3V DC motor functioning as a wind generator producing raw DC power. The acquisition stage employs voltage and current sensors that scale signals to ESP32 ADC input levels. The processing stage utilizes the ESP32 to calculate power (P = V × I) and manage Wi-Fi cloud connectivity. The delivery stage implements high-frequency oscillation in the transmitter coil to induce current in the receiver coil.

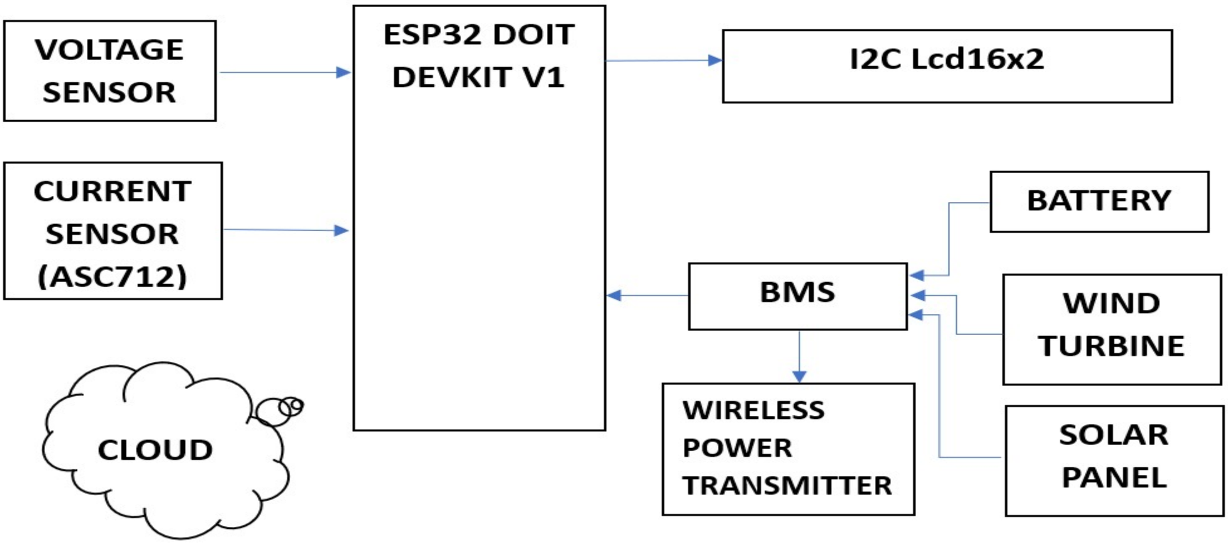

Fig. 1 - Block Diagram of Hybrid Wind-Solar Wireless EV Charging Station Architecture

The combiner circuit merges both sources using Schottky diodes that prevent backflow while minimizing voltage drops. The sensing unit incorporates an ACS712 Hall Effect current sensor providing galvanic isolation and a resistive voltage divider that scales input voltages to the ESP32's 3.3V maximum analog input specification.

B. Mathematical Modeling of Energy Sources

The photo-generated current is directly proportional to incident irradiance:

$$I_p^h = [I_s^c + K_i(T - T_r^{ef})] \times (G / G_r^{ef})$$

The wind generator back-EMF is: $E^g = K^ə \cdot \varphi \cdot \omega$, and mechanical power captured follows: $P^{mech} = \frac{1}{2}\rho A v^3 C_p$, where the Betz limit establishes $C_p \leq 0.593$ for any wind turbine.

C. Wireless Power Transfer Mechanism

The system utilizes Faraday's Law of electromagnetic induction for contactless power delivery. The induced voltage in the receiver coil is: $V_i^{nduked} = -N_2 \times d\Phi/dt$. The coupling coefficient decreases approximately as: $k \approx 1/(1 + (d/r)^3)$, where d is the air gap distance and r is the coil radius, explaining why wireless charging efficiency drops rapidly as distance increases.

D. Sensor Interfacing and Voltage Divider Design

The ESP32 ADC cannot handle voltages exceeding 3.3V. The resistive voltage divider with $R_1 = 30k\Omega$ and $R_2 = 7.5k\Omega$ provides a scaling factor of 5.0:

$$Multiplier = (R_1 + R_2) / R_2 = (30000 + 7500) / 7500 = 5.0$$

$$V^{max} = 3.3V \times 5.0 = 16.5V$$

This provides a safe margin for a 12V solar panel which outputs approximately 14.4V under peak sunlight. The ACS712 Hall Effect sensor outputs an analog voltage proportional to the sensed current with sensitivity of 185 mV/A for the 5A variant, providing 2.1 kV RMS galvanic isolation.

IV. HARDWARE IMPLEMENTATION

A. ESP32 DevKit V1 Microcontroller

The ESP32 DevKit V1 integrates a dual-core Xtensa 32-bit LX6 microprocessor with built-in Wi-Fi and Bluetooth connectivity, operating at clock frequencies up to 240 MHz. The 12-bit ADC maps 0V–3.3V into $2^{12} = 4096$ discrete steps:

$$\Delta V = 3.3V / 4096 \approx 0.806\ mV$$

This resolution is critical for detecting minute changes in current from the 3V wind generator during low-wind conditions. GPIO 35 serves as the analog input for the voltage sensor (resistive divider output), GPIO 34 for the ACS712 current sensor output, and GPIO 21/22 implement I^2C communication for the 16×2 LCD display.

B. Sensing Unit and Circuit Schematic

The ACS712 provides galvanic isolation through the Hall Effect principle, protecting the ESP32 from high-current surges. The 5A variant offers the highest sensitivity of 185 mV/A with a zero-current reference voltage of 2.5V and bandwidth exceeding 80 kHz. The complete circuit schematic below shows all interconnections between components including the parallel connection of the solar panel and wind motor via blocking Schottky diodes.

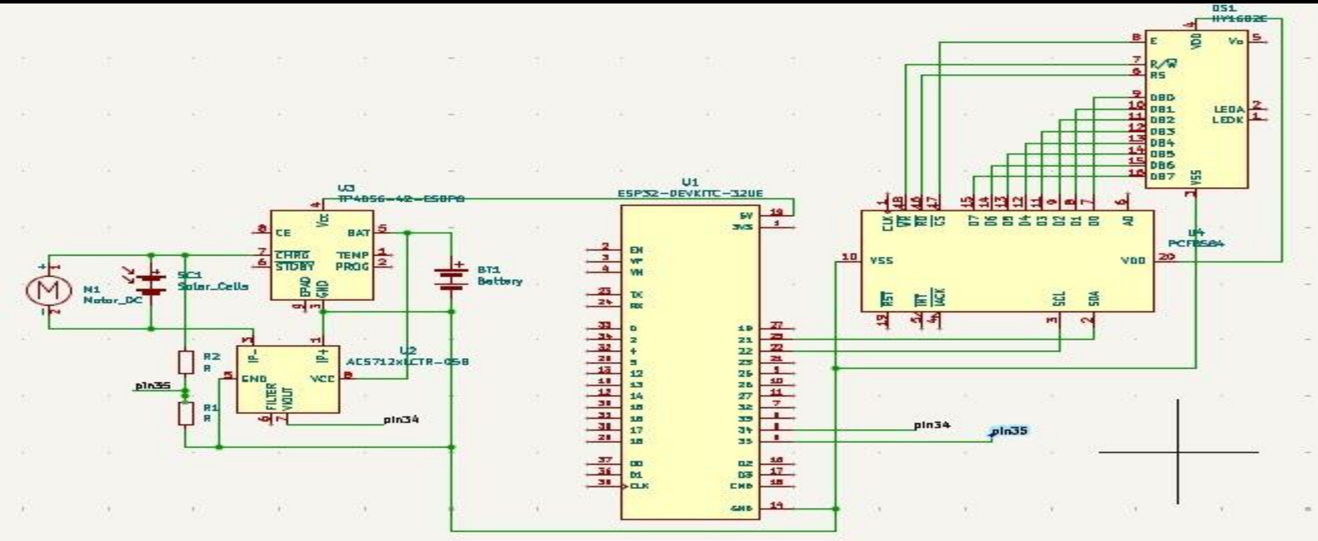

Fig. 2 - Complete Circuit Schematic of the Hybrid EV Charging Station

C. Wireless Transmitter-Receiver Module

The wireless power transfer module facilitates contactless EV charging. The transmitter generates an alternating current at 100–200 kHz, creating a time-varying magnetic field. The receiver consists of a secondary coil and rectification circuit. The coil inductance is: $L = \mu_o N^2 A/l$. Experimental results demonstrate 75% power transfer efficiency at an optimal air gap of 5mm. As distance increases to 15mm, efficiency decreases to approximately 45%, demonstrating the cubic distance dependence of inductive coupling.

V. SOFTWARE DEVELOPMENT AND IOT INTEGRATION

A. Firmware Architecture

The firmware for the ESP32 was developed using the Arduino IDE utilizing libraries: WiFi.h for network stack management, BlynkSimpleEsp32.h for cloud synchronization, and LiquidCrystal_I2C.h for the display interface. Compiler settings were configured for ESP32 Dev Module at 240 MHz CPU frequency.

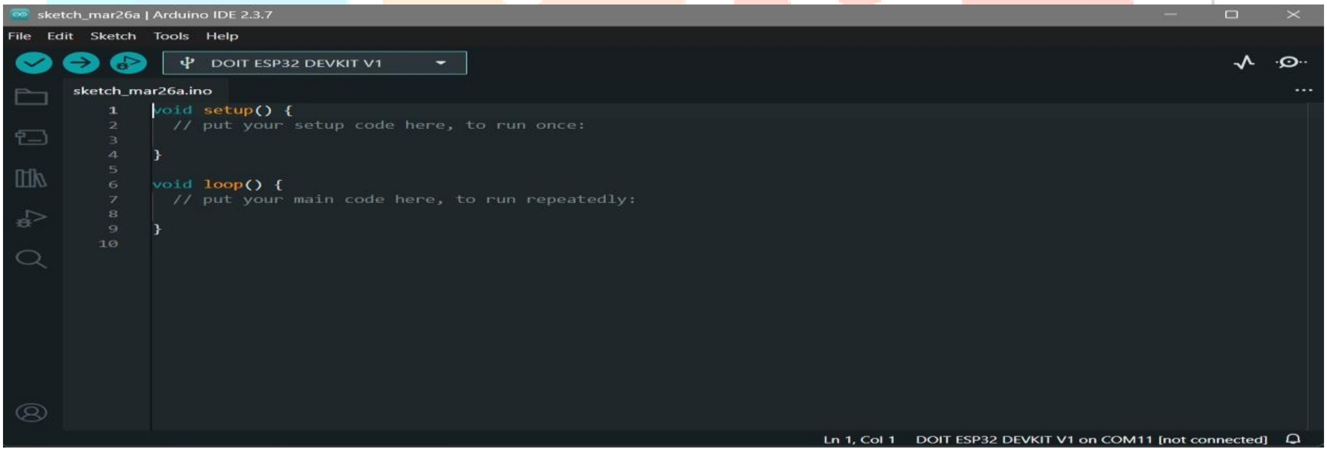

Fig. 3 - Arduino IDE Programming Environment

The software follows a non-blocking timer-driven architecture. A BlynkTimer object triggers the sendSensorData() function every 1000 milliseconds, allowing the main loop to continuously service the Wi-Fi stack and Blynk protocol without blocking.

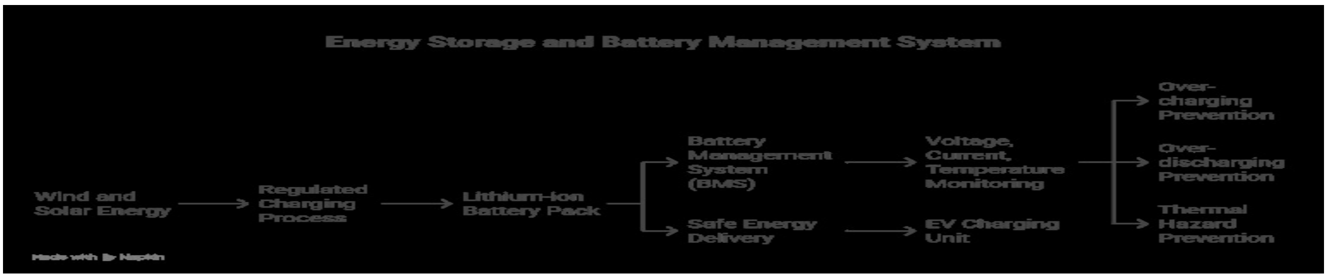

Fig. 4 - System Firmware Flowchart

The voltage scaling applies the multiplier from the resistor divider ratio: $V^{actual} = V^{mea}{}_{s}{}^{uRed} \times 5.0$. A conditional check prevents ghost current readings when the system is powered down. A rolling average filter smooths wind generator output spikes using: $\bar{x}_n = (1/N)\Sigma\, x_{n-i}$ for N samples.

B. Blynk IoT Platform Integration

Blynk IoT Version 2.0 provides a visual programming environment for custom dashboards. Virtual Pin V0 transmits calculated voltage (after divider scaling), V1 transmits calibrated current, and V2 transmits computed wattage (P = V × I). The dashboard features three gauge widgets for instantaneous readings and three SuperChart widgets visualizing real-time trends over selectable intervals of 1 hour, 1 day, and 1 week.

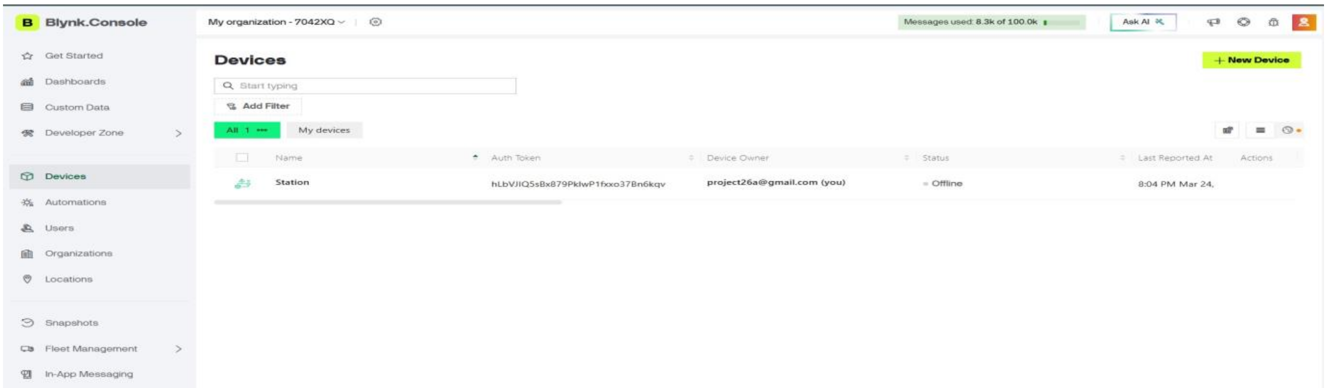

Fig. 5 - Blynk IoT Cloud Dashboard

Security is provided through the BLYNK_AUTH_TOKEN, a 32-character alphanumeric string authenticating the device to Blynk cloud servers, preventing unauthorized access to the data stream. The ESP32 Wi-Fi stack includes automatic reconnection features ensuring continuous telemetry even during network interruptions.

VI. RESULTS AND DISCUSSION

A. Experimental Setup

The experimental setup was conducted in a controlled outdoor-indoor environment. A 12V/10W polycrystalline solar panel was placed under direct sunlight with average irradiance measured at 800 W/m². A 3V DC generator motor with a three-blade turbine was subjected to wind speeds between 2 m/s and 8 m/s using a regulated blower. Data was logged simultaneously on the 16×2 I²C LCD and the Blynk IoT Cloud.

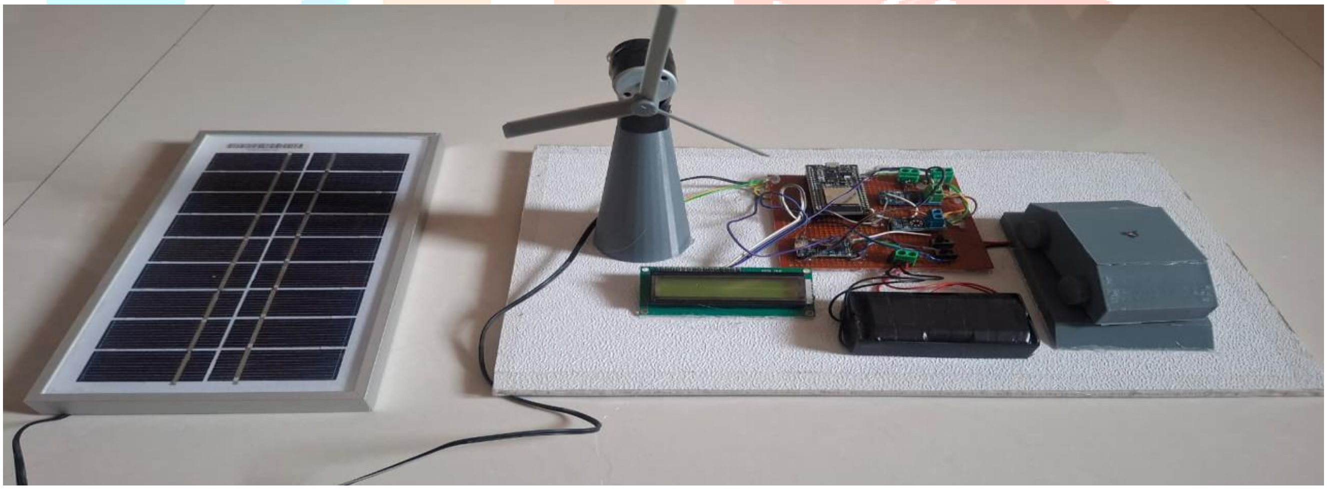

Fig. 6 - Experimental Hardware Setup

B. Real-Time Monitoring and Analysis

The Blynk dashboard voltage trend starts from a baseline of 0.70V (cut-in threshold) and climbs to a stable peak between 1.87V and 2.03V. The current remains remarkably consistent at 0.151A with minimal variation (spikes to 0.152A, dips to 0.149A), demonstrating excellent current regulation due to the impedance characteristics of the inductive coupling system. Real-time power is recorded at 0.28W, verified as:

$$P = V \times I = 1.87V \times 0.151A = 0.282W \approx 0.28W$$

Fig. 7 (Left) & Fig. 8 (Right) - Blynk App Real-Time Monitoring Output

C. Performance Evaluation of Hybrid Source

The hybrid configuration was tested by evaluating solar-only, wind-only, and combined operation. During solar-only operation, the system provided steady but lower current (< 100 mA) during cloudy intervals. During wind-only testing, the generator output exhibited greater variability with peak instantaneous power reaching 0.20W but average only 0.12W. When both sources operate in hybrid mode, the system reaches 2.03V peak faster and maintains voltage more consistently, demonstrating the complementary nature of the two generation sources.

D. Wireless Charging Efficiency and Comparative Analysis

Wireless power transfer efficiency was highest at approximately 75% at a 5mm air gap. At 15mm, efficiency decreased to approximately 45%. The efficiency is defined as: $\eta = (P_{out} / P_{in}) \times 100\%$.

Table 1 - Theoretical vs. Experimental Results Comparison

Parameter	Theoretical	Experimental	Deviation (%)
Voltage (V)	2.10	1.87–2.03	10.9%
Current (A)	0.160	0.151	5.6%
Power (W)	0.336	0.28	16.6%
WPT Efficiency	85%	75%	11.8%

The voltage deviation of 10.9% is attributed to the internal resistance of the 3V motor, forward voltage drops across blocking diodes (0.3V–0.7V), and contact resistances in connectors and PCB traces. The current deviation of 5.6% is minimal, proving the ACS712 and ESP32 ADC calibration are highly accurate. The power deviation of 16.6% is larger because power is the product of voltage and current, causing errors to compound.

VII. CONCLUSION

This research successfully demonstrated the design and implementation of an IoT-enabled hybrid wind-solar electric vehicle charging station. By integrating a solar PV panel and a 3V wind generator motor, a multi-source power system was established to mitigate renewable energy intermittency. The ESP32 DevKit V1 served as the central telemetry unit, acquiring data via the ACS712 current sensor and a precision voltage divider ($R_1 = 30k\Omega$, $R_2 = 7.5k\Omega$), providing real-time visualization through I^2C LCD and remote monitoring via Blynk IoT Cloud.

Key conclusions: (i) The combined solar and wind input provided a more stable voltage profile (1.87V–2.03V) compared to standalone sources; (ii) The 12-bit ADC of the ESP32 maintained steady current reading of 0.151A with minimal noise; (iii) The Blynk platform successfully logged data over weekly and monthly intervals, demonstrating suitability for long-term telemetry; (iv) Wireless transmission efficiency is highly distance-sensitive, with 5mm air gap found optimal for 0.28W delivery. Future work includes implementation of MPPT algorithms (20–30% improvement in energy harvest), Vehicle-to-Grid bidirectional power flow, resonant inductive coupling for larger air gaps, and machine learning-based prediction of renewable generation from weather forecasts.

ACKNOWLEDGMENT

The authors express sincere gratitude to Dr. A.V. Mohod (Guide), Dr. K.S. Panpaliya (Co-Guide), and Dr. S.B. Mohod, Dean (PG Studies), Department of Electrical Engineering, Prof. Ram Meghe College of Engineering & Management, Badnera-Amravati, for their invaluable guidance and support throughout this research work. The authors also thank the Principal Dr. A.P. Thakare for providing necessary facilities.

REFERENCES

[1] S. Chopra and R. Kumar, "Wireless Power Transfer for Electric Vehicles: A Review," IEEE Transactions on Power Electronics, vol. 38, no. 2, pp. 1120–1135, 2024.

[2] Blynk IoT Documentation, "Integrating ESP32 with Virtual Pins for Real-time Telemetry," [Online]. Available: https://docs.blynk.io.

[3] J. Ibrahim, "Solar-Wind Hybrid Systems in Urban Environments," Renewable Energy Journal, vol. 15, pp. 201–210, 2023.

[4] M. Chen and L. Wang, "Maximum Power Point Tracking Algorithms for Photovoltaic Systems," IEEE Transactions on Sustainable Energy, vol. 9, no. 4, pp. 1856–1867, 2018.

[5] R. Patel and S. Gupta, "Hall Effect Current Sensors for Power Electronics Applications," Sensors and Actuators A: Physical, vol. 285, pp. 612–620, 2019.

[6] K. Lee and H. Kim, "Inductive Power Transfer for Electric Vehicle Charging: A Survey," IEEE Access, vol. 8, pp. 147924–147945, 2020.

[7] T. Nakamura and Y. Tanaka, "Small-scale Wind Energy Conversion Systems for Urban Applications," Renewable Energy, vol. 145, pp. 1250–1262, 2020.

[8] D. Anderson and M. Thompson, "Internet of Things Platforms for Energy Management," IEEE Internet of Things Journal, vol. 7, no. 6, pp. 5012–5025, 2020.

[9] F. Garcia and J. Martinez, "Vehicle-to-Grid Technology: Challenges and Opportunities," Applied Energy, vol. 267, 114902, 2020.